Supplementary Materials

3D-Printed Highly Stretchable Conducting Polymer Electrodes for Flexible Supercapacitors

Jiayu Yang,[a] Qinghe Cao,[a] Xiaowan Tang,[a] Junjie Du,[a] Tao Yu,[a*] Xi Xu,[a] Dongming Cai,[b] Cao Guan[a*] and Wei Huang[a]

[1]Frontiers Science Center for Flexible Electronics, Institute of Flexible Electronics, Northwestern Polytechnical University, Xi'an 710072, P. R. China
E-mail: iamtyu@nwpu.edu.cn; iamcguan@nwpu.edu.cn .

[2]College of Chemical Engineering, Hubei University, Wuhan 430062, P. R. China

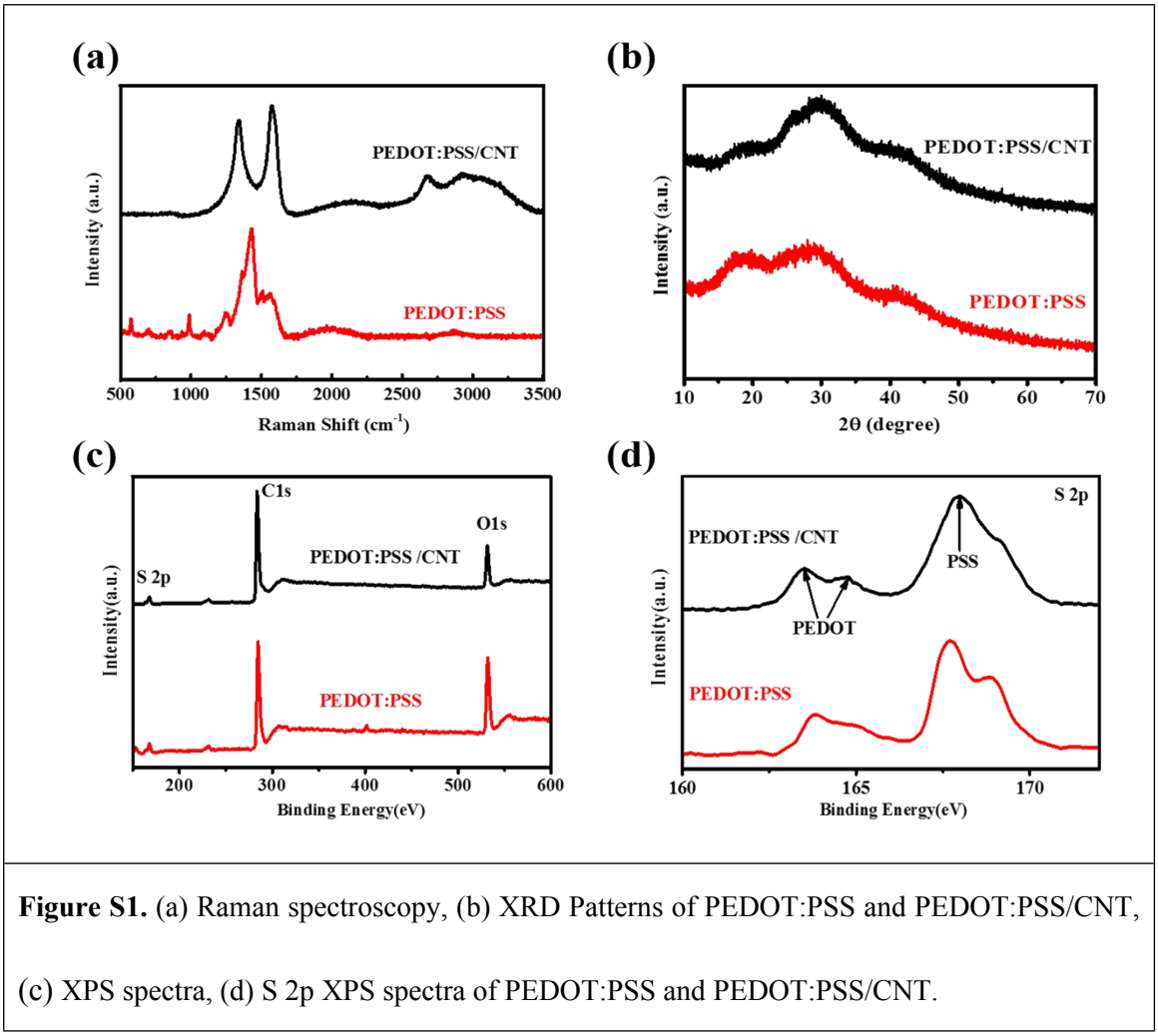

Figure S1. (a) Raman spectroscopy, (b) XRD Patterns of PEDOT:PSS and PEDOT:PSS/CNT, (c) XPS spectra, (d) S 2p XPS spectra of PEDOT:PSS and PEDOT:PSS/CNT.

Fig. S1 (Supporting Information) depicts the characterization of the PEDOT:PSS and PEDOT:PSS/CNT. The Raman spectra of PEDOT:PSS and PEDOT:PSS/CNT are shown in Fig. S1a. The PEDOT:PSS exhibits a remarkable band at 1442 cm^{-1}, corresponding to Cα=Cβ stretching vibration from thiophene rings. The PEDOT:PSS/CNT with two major bands at 1345 and 1596 cm^{-1}, corresponding to the D and G bands, respectively, which can be attributed to the disorders and defects in CNT[1]. Fig. S1b shows that both PEDOT:PSS and PEDOT:PSS/CNT have two broad peaks due to their intrinsic amorphism at 2Θ=18.5° and 2Θ=26.5°, which can be attributed to the thiophene p–p stacking of PEDOT and benzene p–p stacking of PSS, respectively. Moreover, the diffraction intensity of PEDOT:PSS/CNT at 2Θ=18.5° is

weaker than that of PEDOT:PSS. Compared to the peaks of PEDOT:PSS, the CNT in PEDOT:PSS/CNT is not obvious[2, 3].

The XPS scan of the PEDOT:PSS and PEDOT:PSS/CNT is shown in Fig. S1c. The C, O and S peaks confirm the PEDOT:PSS on the surface that indicate the uniformity of the composite. The region scans of S is shown in Fig. S1d, the 164.2 and 165.2 eV peaks are attributed to the thiophene groups in PEDOT. The 168.1 and 169.2 eV peaks are due to the sulfonate groups in PSS. The above results demonstrated the successful synthesis of PEDOT:PSS and PEDOT:PSS/CNT[4-8].

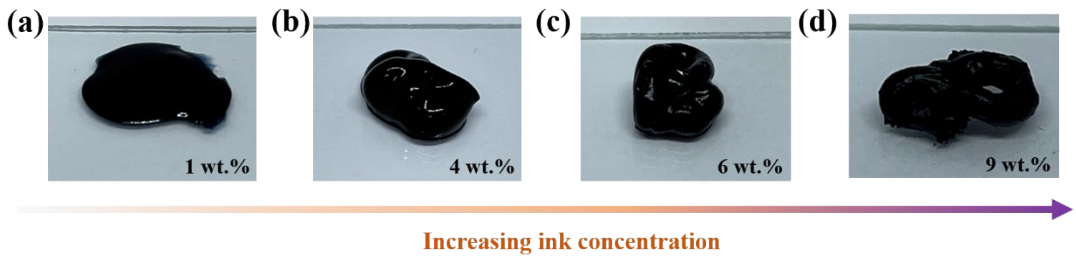

Figure S2. Images of conducting polymer ink with varying concentration.

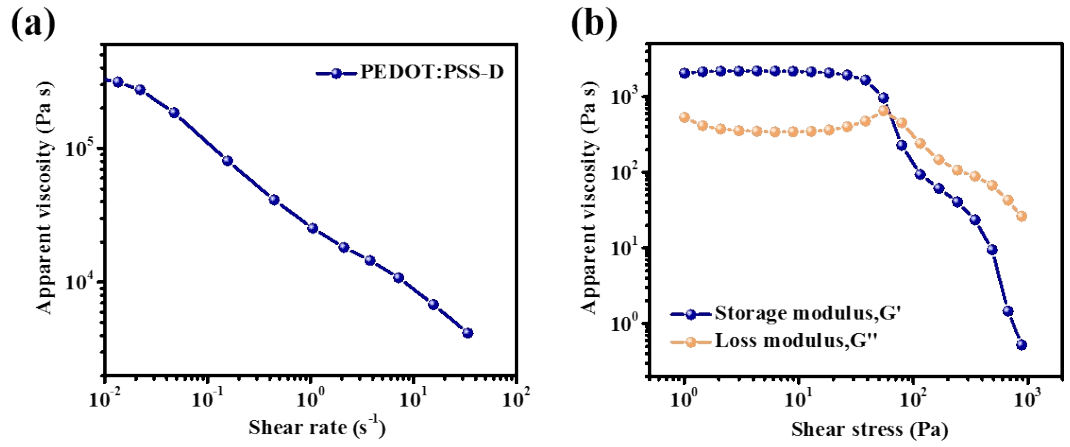

Figure S3. (a) Apparent viscosity as a function of shear rate for PEDOT:PSS-D ink, (b) The storage modulus, G′, and loss modulus, G″, as a function of shear stress for PEDOT:PSS-D ink.

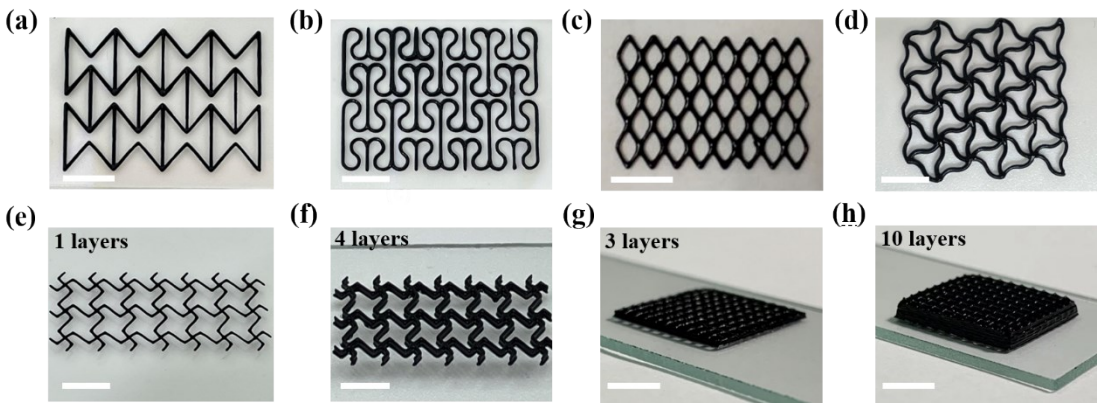

Figure S4. a-d) Images of as-printed electrodes with different Negative Poisson's Ratio (NPR) structures before freeze-drying. e,f) Images of 3D-printed electrodes with different layer thicknesses of chiral structure. g,h) Images of 3D-printed conducting polymer mesh with different layer thicknesses. Scale bars, 5 mm (a-h).

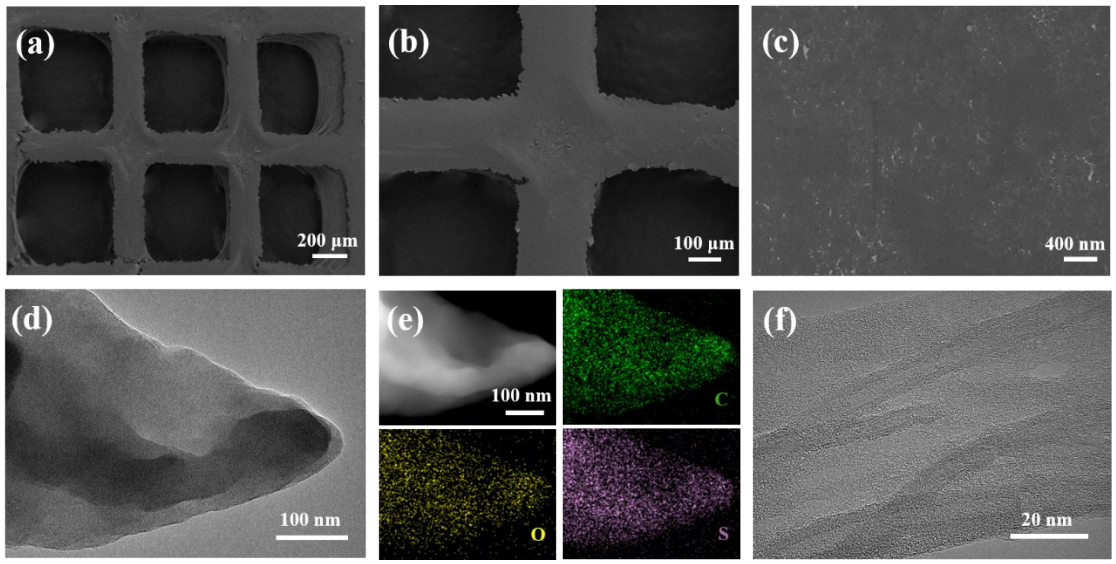

Figure S5. Morphology characterizations of both the 3D-printed PEDOT:PSS-D and PEDOT:PSS/CNT frameworks. a-e) Typical characterization of 3D-printed PEDOT:PSS-D. a-c) SEM images. d) TEM image. e) elemental mapping images of C, O, and S for 3D-printed PEDOT:PSS-D framework. f) HRTEM image 3D-printed PEDOT:PSS/CNT framework.

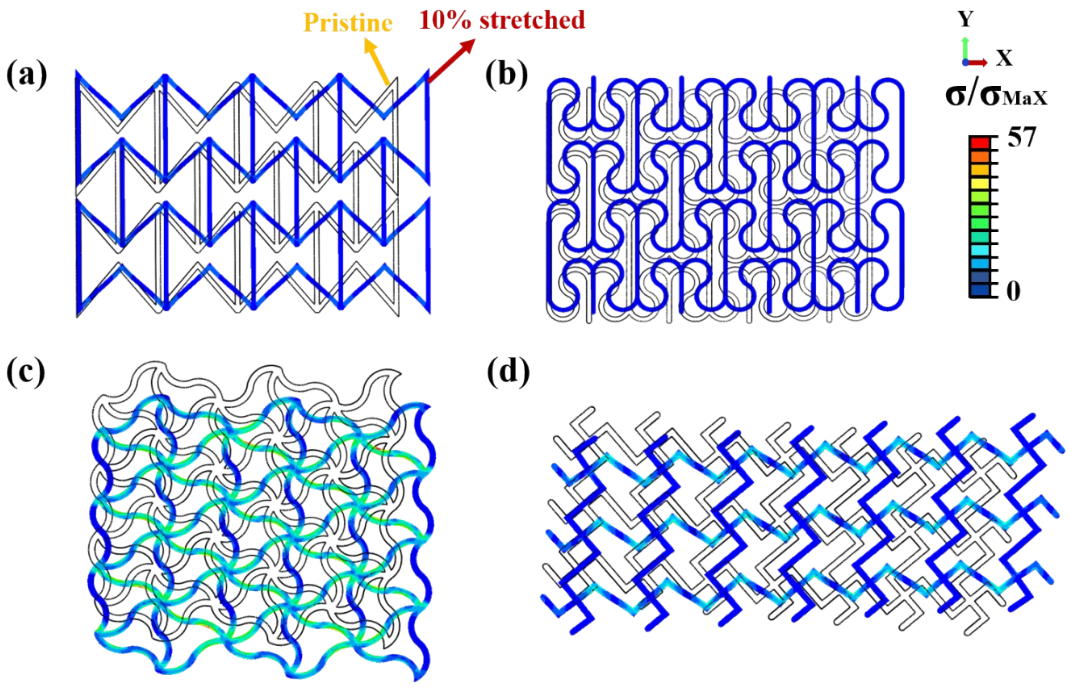

Figure S6. The von Mises stress distribution in the electrodes with four different NPR structures at 10% stretched state.

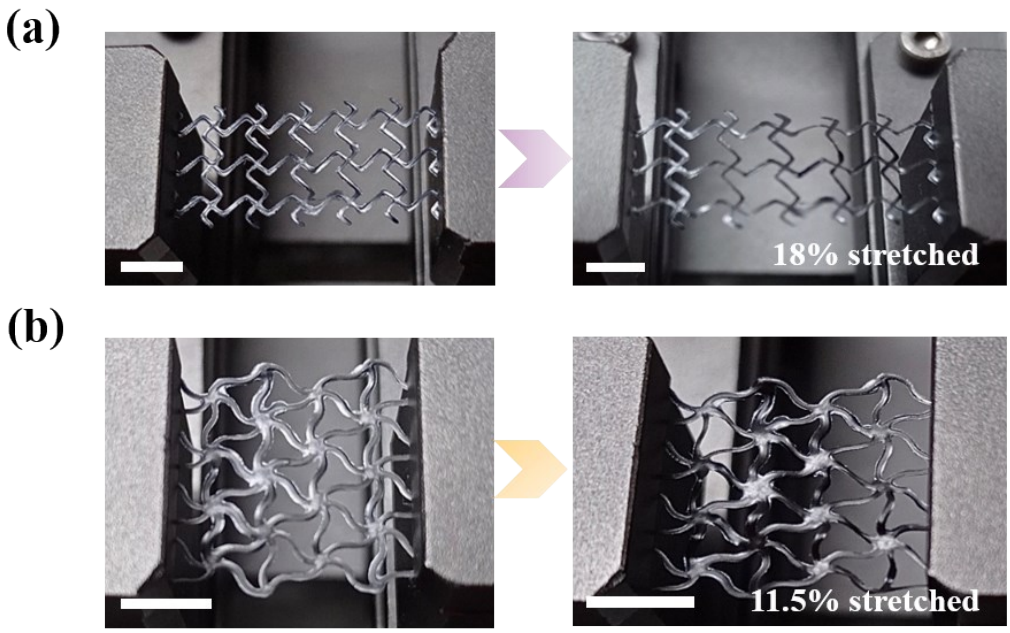

Figure S7. The optical images of a) Chiral and b) Wavy mesh structure electrodes in maximum stretch state. Scale bars: 5 mm.

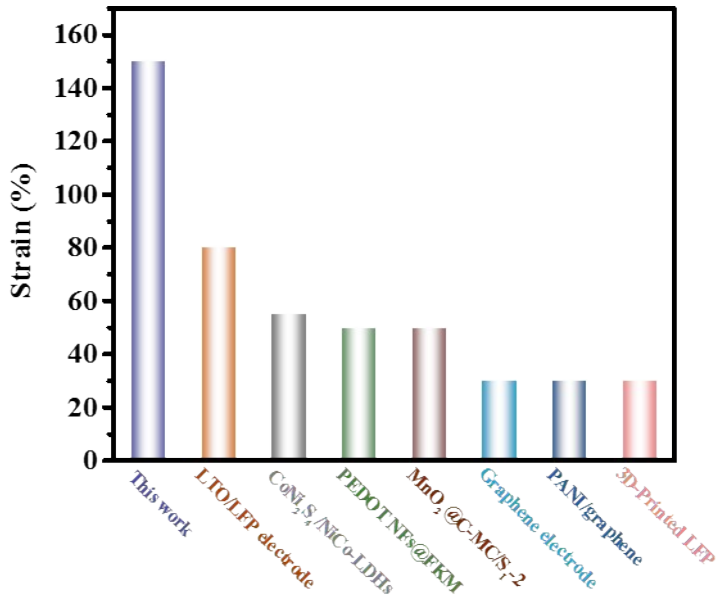

Figure S8. A plot compares the ultimate tensile rate of the 3D-printed conductingpolymer-based electrode with the values of previously reported stretchable electrodes (LTO/LFP[9], $CoNi_2S_4$/NiCo-LDHs[10], PEDOT NFs@FKM[11], MnO_2@C-MC/S_1-2[12], graphene electrode[13], PANI/graphene[14], 3D-printed LFP[15].

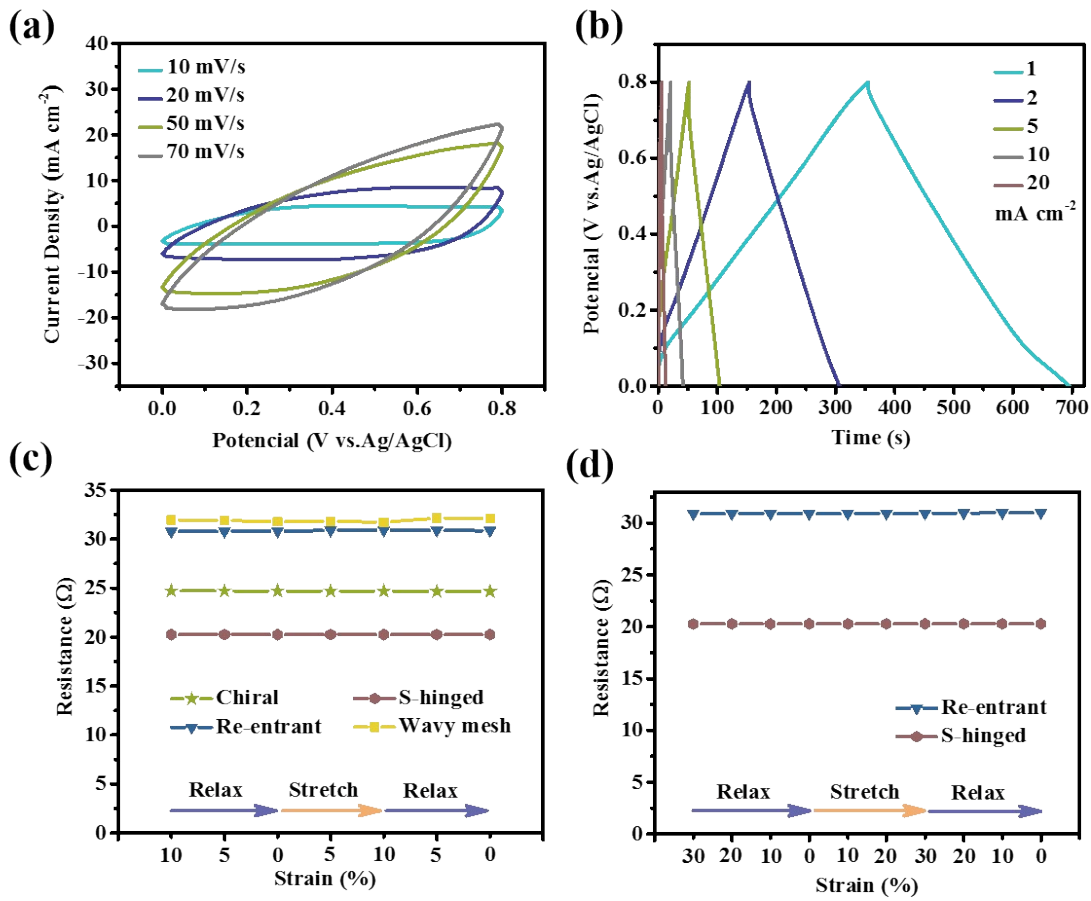

Figure S9. Mechanical and electrical characterization of the 3D-printed conducting polymer-based electrode. a) CV curves of PEDOT:PSS electrode at scan rates from 10 to 70 mV s^{-1}. b) GCD curves of PEDOT:PSS electrode at various current densities ranging from 1 to 20 mA cm^{-2}. c) Variations of the electrical resistances of the 3D-printed conducting polymer-based electrode with different NPR structures as a function of applied stretching strains from 0 to 10%. d) Variations of the electrical resistances of the 3D-printed conducting polymer-based electrode with Re-entrant and S-hinged structures as a function of applied stretching strains from 0 to 30%.

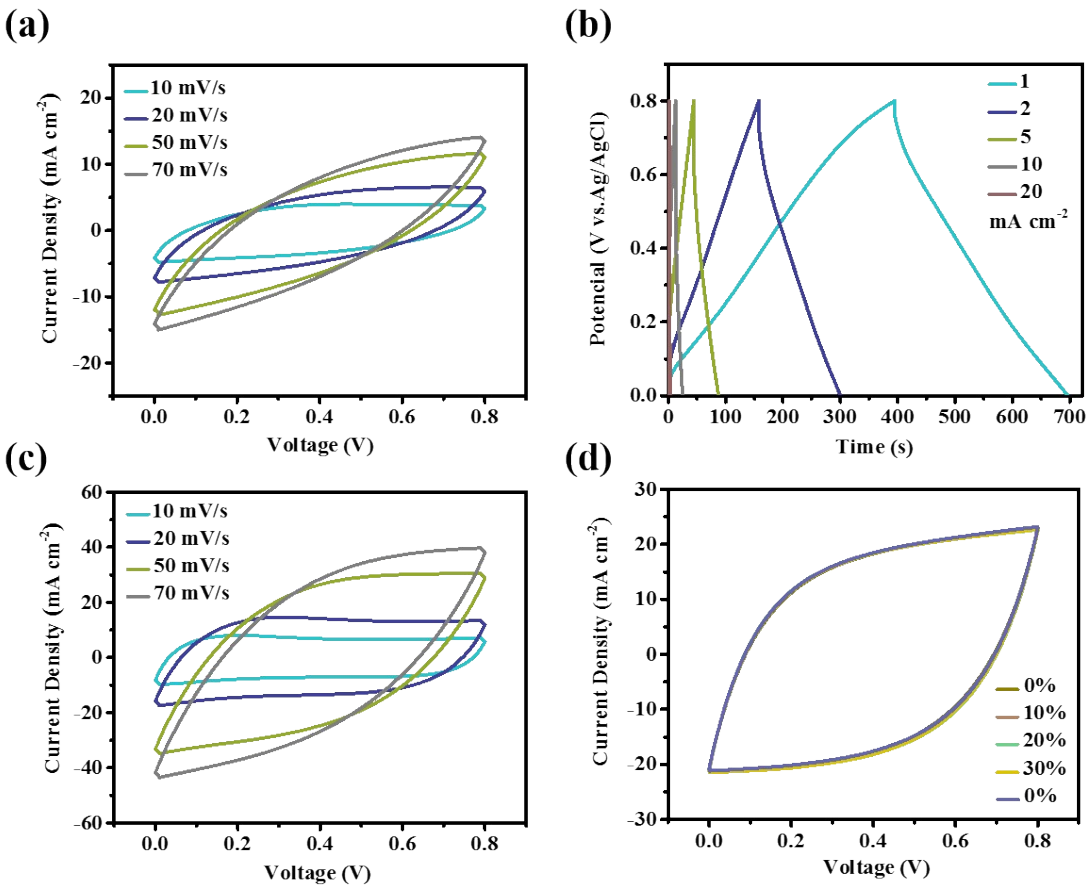

Figure S10. Electrochemical characterizations of 3D-printed PEDOT:PSS and PEDOT:PSS/CNT supercapcitor. a) CV curves of the assembled PEDOT:PSS SSC at different scan rates. b) GCD curves of PEDOT:PSS SSC with different current densities. c) CV curves of the assembled PEDOT:PSS/CNT SSC at different scan rates. d) CV curves of the stretchable SC at 30 mV/s scan rate under different stretching strains.

Reference

1. N. Kurra, J. Park and H. N. Alshareef, J. Mater. Chem. A, 2014, 2, 17058-17065.
2. N. Kim, S. Kee, S. H. Lee, B. H. Lee, Y. H. Kahng, Y. R. Jo, B. J. Kim and K. Lee, Adv. Mater., 2014, 26, 2268-2272.
3. G. Cai, P. Darmawan, M. Cui, J. Wang, J. Chen, S. Magdassi and P. S. Lee, Adv. Energy Mater., 2016, 6, 1501882.
4. W. Yan, J. Li, G. Zhang, L. Wang and D. Ho, J. Mater. Chem. A, 2020, 8, 554-564.
5. Y. Zeng, Y. Han, Y. Zhao, Y. Zeng, M. Yu, Y. Liu, H. Tang, Y. Tong and X. Lu, Adv. Energy Mater., 2015, 5, 1402176.
6. T. G. Yun, M. Park, D. H. Kim, D. Kim, J. Y. Cheong, J. G. Bae, S. M. Han and I. D. Kim, ACS Nano, 2019, 13, 3141-3150.
7. Z. Su, C. Yang, C. Xu, H. Wu, Z. Zhang, T. Liu, C. Zhang, Q. Yang, B. Li and F. Kang, J. Mater. Chem. A, 2013, 1, 12432–12440.
8. V. R. Feig, H. Tran, M. Lee, K. Liu, Z. Huang, L. Beker, D. G. Mackanic and Z. Bao, Adv. Mater., 2019, 31, 1902869.
9. W. Liu, Z. Chen, G. Zhou, Y. Sun, H. R. Lee, C. Liu, H. Yao, Z. Bao and Y. Cui, Adv.Mater., 2016, 28, 3578-3583.
10. P. Chang, H. Mei, Y. Tan, Y. Zhao, W. Huang and L. Cheng, J. Mater. Chem. A, 2020, 8, 13646-13658.
11. H. Mu, W. Wang, L. Yang, J. Chen, X. Li, Y. Yuan, X. Tian and G. Wang, Energy Storage Mater., 2021, 39, 130-138.
12. X. Li, J. Wang, K. Wang, J. Yao, H. Bian, K. Song, S. Komarneni and Z. Cai, Chem. Eng. J., 2020, 390, 124442.
13. J. Y. Hong, W. Kim, D. Choi, J. Kong and H. S. Park, ACS Nano, 2016, 10, 9446-9455.
14. Y. Xie, Y. Liu, Y. Zhao, Y. H. Tsang, S. P. Lau, H. Huang and Y. Chai, J. Mater. Chem. A, 2014, 2, 9142-9149.
15. Y. Bao, Y. Liu, Y. Kuang, D. Fang and T. Li, Energy Storage Mater., 2020, 33, 55-61.